Research Square

Preprints are preliminary reports that have not undergone peer review.
They should not be considered conclusive, used to inform clinical practice,
or referenced by the media as validated information.

Gait-phase-dependent neural dynamics differ between treated Parkinson's disease and healthy controls

Lena Salzmann

relab.publications@hest.ethz.ch

ETH Zurich

Aline S. Brunner

ETH Zurich

Zhongke Mei

ETH Zurich

Andreas Fleisch

University Hospital Zurich

William R. Taylor

ETH Zurich

Victoria Peterson

Universidad Nacional del Litoral

Lukas Imbach

Swiss Epilepsy Center

Deepak K. Ravi

ETH Zurich

Olivier Lambercy

ETH Zurich

Roger Gassert

ETH Zurich

Article

Keywords:

Posted Date: September 17th, 2026

DOI: https://doi.org/10.21203/rs.3.rs-10919819/v1

License: This work is licensed under a Creative Commons Attribution 4.0 International License.
Read Full License

Additional Declarations: Competing interest reported. L.I. has received honoraria for lectures, advisory board participation, or consulting from UCB, Eisai, and Medtronic (all not related to this work). The remaining authors declare no competing interests.

Gait-phase-dependent neural dynamics differ between treated Parkinson's disease and healthy controls

Lena Salzmann[1*†], Aline S. Brunner[1†], Zhongke Mei[2], Andreas Fleisch[3], William R. Taylor[2], Victoria Peterson[4], Lukas Imbach[5, 6], Deepak K. Ravi[2], Olivier Lambercy[1], Roger Gassert[1]

[1*]Rehabilitation Engineering Laboratory, ETH Zurich, Gloriastrasse 37/39, 8092, Zurich, Switzerland.
[2]Laboratory for Movement Biomechanics, ETH Zurich, Gloriastrasse 37/39, 8092, Zurich, Switzerland.
[3]Neurology, University Hospital Zurich, Frauenklinikstrasse 26, 8091, Zurich, Switzerland.
[4]Instituto de Matemática Aplicada del Litoral, CONICET-UNL, Colectora Ruta Nac. 168, Paraje El Pozo, 3000, Santa Fe, Argentina.
[5]Swiss Epilepsy Centre, Klinik Lengg, Bleulerstrasse 60, 8008, Zurich, Switzerland.
[6]Institute for Neuroscience, ETH Zurich, Gloriastrasse 37/39, 8092, Zurich, Switzerland.

*Corresponding author(s). E-mail(s): relab.publications@hest.ethz.ch;
Contributing authors: aline.brunner@hest.ethz.ch; zhongke.mei@hest.ethz.ch; andreas.fleisch@usz.ch; bt@ethz.ch; vpeterson@imal.unl.edu.ar; lukas.imbach@kliniklengg.ch; deepak.ravi@hest.ethz.ch; olivier.lambercy@hest.ethz.ch; roger.gassert@hest.ethz.ch;
†These authors contributed equally to this work.

Abstract

Gait disturbances in Parkinson's disease (PD) often persist despite dopaminergic medication and subthalamic nucleus deep brain stimulation (STN-DBS), yet

the neural activity accompanying gait under combined therapy remains incompletely understood. We recorded mobile electroencephalography (EEG), STN local field potentials (PD only), and motion capture during overground walking in 10 individuals with PD under combined STN-DBS and dopaminergic therapy and 10 age-matched healthy controls (HC). Overall spectral characteristics showed few PD–HC differences and no significant rest-versus-walking differences in STN parameters. Gait-phase-resolved analyses, however, revealed an altered temporal organisation of neural activity: cortical gait-phase modulation differed between PD and HC, most clearly in prefrontal high-beta and gamma, and STN low-beta, high-beta, and gamma activity was modulated across the gait cycle, with hemisphere-by-gait-phase interactions in theta and gamma. Gait-related biomarkers and neuromodulation may therefore benefit from capturing the temporal organisation of neural dynamics across the gait cycle rather than average spectral magnitude alone.

Introduction

Parkinson's disease (PD) is the second most prevalent neurodegenerative disorder worldwide and is characterised by the progressive loss of dopaminergic neurons within the basal ganglia, resulting in motor symptoms including bradykinesia, rigidity, tremor, and disturbances of gait and postural control [1]. Among these symptoms, gait impairments are particularly disabling because they directly affect mobility and independence and often become increasingly difficult to manage as the disease progresses. Dopaminergic medication and deep brain stimulation (DBS) of the subthalamic nucleus (STN) effectively alleviate several cardinal motor symptoms of PD, yet gait impairments can persist despite optimised therapy [2–4]. This incomplete therapeutic response suggests that the neural activity underlying gait may not be fully restored even when individuals are examined in their standard therapeutic (ON) state. Characterising these persistent alterations in neural activity during gait may therefore provide insight into the mechanisms underlying residual gait dysfunction in PD under combined dopaminergic and DBS treatment (hereafter treated PD).

PD is associated with altered neural oscillations throughout cortico-basal ganglia circuits. Local field potentials (LFPs) recorded from the STN consistently show pathological synchronisation, particularly within the beta frequency range, which is associated with bradykinesia and rigidity [5, 6]. Abnormal oscillatory activity is, however, not confined to the STN. Although findings regarding cortical oscillations are more heterogeneous, altered cortical activity and cortico-subcortical interactions have also been reported in PD [7–11]. Both dopaminergic medication and DBS attenuate pathological oscillatory activity across this wider cortico-basal ganglia network and improve motor performance [12–14]. Together, these findings establish abnormal oscillatory activity as an important feature of PD pathophysiology and show that it can be substantially modified by treatment. However, attenuation of pathological spectral activity does not necessarily indicate that the physiological temporal organisation of neural activity required for gait has been restored.

Physiological movement is characterised not only by changes in average oscillatory power, but also by dynamic modulation of neural activity in relation to movement execution. Cortically, movement is accompanied by event-related desynchronisation (ERD) of alpha and beta activity and increases in higher-frequency gamma activity [15–17]. During natural gait, these oscillations are further modulated across the gait cycle: healthy individuals exhibit rhythmic, gait-phase-locked modulation, including alpha and beta desynchronisation during limb swing and partial resynchronisation around stance and double-support phases, together with gait-phase-dependent gamma activity around specific stance events [18–21]. In PD, these physiological patterns are altered. Under dopaminergic medication alone (ON-medication state), stronger ERD across theta, alpha, and low-beta bands has been reported over the whole gait cycle, together with weakened gait-phase-locked cortical modulation [22]. Even under levodopa treatment, reduced movement-related alpha and beta desynchronisation has been observed over motor cortical regions, including the supplementary motor area, during upper-limb movement [23, 24]. It nevertheless remains unclear whether the gait-phase-locked cortical modulation disrupted in PD is normalised or persists under combined dopaminergic treatment and DBS.

A similar distinction between overall spectral activity and movement-related temporal modulation applies to the STN. Whereas cortical activity can be assessed non-invasively in both healthy individuals and people with PD, direct recordings of subthalamic activity are restricted to patients implanted with DBS electrodes. During upper-limb movements, STN activity shows movement-related beta desynchronisation in the off-treatment state [25], and this modulation is altered by combined dopaminergic treatment and DBS [12]. During gait, STN beta activity is likewise dynamically modulated: beta peak frequency varies with walking [26], and gait-related beta suppression relative to rest has been observed in PD off treatment, particularly in the high-beta range [4, 27, 28]. This rest-to-gait beta suppression is less apparent in the ON-stimulation state [27]. Beyond these overall spectral changes, STN activity also varies across the gait cycle, while PD off treatment has been associated with reduced gait-phase-locked subthalamic modulation [4, 26]. These findings indicate that changes in overall STN oscillatory activity and changes in its modulation across the gait cycle reflect distinct aspects of treatment-related neural dynamics.

Despite this evidence, it remains unclear how cortical and subthalamic gait-related dynamics are expressed when patients receive combined STN-DBS and dopaminergic treatment. Most previous electrophysiological studies of gait in PD have characterised patients in the off-treatment state, investigated individual treatment modalities, or lacked a direct comparison with age-matched healthy controls (HC); a recent study that did include a healthy-control comparison focused on gait kinematics rather than the underlying neural dynamics [29]. Recent advances in mobile electrophysiology now permit simultaneous recording of cortical electroencephalography (EEG), subthalamic LFPs, and movement kinematics during natural behaviour such as overground walking, providing an opportunity to address this gap.

The present study therefore investigated cortical and subthalamic neural activity during gait in people with PD receiving combined STN-DBS and dopaminergic therapy. We examined whether cortical activity remained altered relative to age-matched

HC, while simultaneously characterising subthalamic activity in the treated PD group. Simultaneous mobile EEG, STN-LFP, and motion-capture data were acquired during overground walking to characterise neural activity at two complementary temporal scales: its overall spectral characteristics averaged across walking, and its modulation within the gait cycle. First, power spectral density (PSD), including its periodic and aperiodic components, was used to assess overall spectral characteristics at rest and during walking. Second, gait-event-related spectral perturbations (gERSPs) and the resulting Gait-Event-Related De/Synchronisation (gERD/ERS) patterns were used to quantify the temporal modulation of oscillatory activity across the gait cycle. Together, these complementary analyses distinguished overall spectral characteristics from the temporal organisation of neural activity during gait. We hypothesised that differences in cortical gait-related neural activity between treated PD and HC would persist, particularly in the temporal modulation of oscillatory activity across the gait cycle.

Results

An overview of the experimental setup, neural read-outs, and main findings is provided in Fig. 1. PD participants were assessed ON dopaminergic medication and ON DBS, i.e. with both therapies active at their individually optimised, stable clinical settings (STN-DBS implanted at least one year before enrolment; see Methods). Cortical EEG (both cohorts) and unilateral STN-LFP activity (PD only, recorded contralateral to the symptom-dominant body side; see Methods) were recorded during both rest and overground walking, with gait events derived from synchronised motion capture and the gait cycle divided into four phases: initial double support (IDS), left leg swing (LLS), final double support (FDS), and right leg swing (RLS). Spectral activity was assessed using PSD, while gait-phase-dependent modulation was quantified using gERSPs and gERD/ERS. Fig. 1 summarises the complementary analyses and the main pattern of results described below.

On average, 91.1 ± 24.0 gait cycles per participant remained for analysis after removing 8.2% of segmented epochs as artefact-contaminated (per-subject counts in Supplementary Tab. S1).

Cortical spectral characteristics show few but significant differences between PD and HC

Cortical PSDs for the prefrontal and motor cortex at rest and during walking are shown in Fig. 2 (prefrontal ROI: channels AF3, F1, Fz, F2, AF4; motor ROI: C3, C1, Cz, C2, C4; see Methods). All spectral parameters derive from the fitting-oscillations-and-one-over-f (FOOOF) parameterisation of the PSDs into periodic and aperiodic components (see Methods). For periodic parameters (peak power and centre frequency), two between-cohort differences survived correction of the false discovery rate (FDR; Benjamini–Hochberg procedure; Tab. 1): during walking, PD showed higher prefrontal alpha power than HC ($p_{\text{raw}} = 0.003$, $p_{\text{FDR}} = 0.035$), and at rest, motor high-beta centre frequency was lower in PD than HC (Welch $t = -4.85$, mean difference $= -4.474$ Hz, $p_{\text{raw}} < 0.001$, $p_{\text{FDR}} = 0.004$). Other between-cohort effects did not survive FDR correction. Aperiodic parameters (exponent and offset) did not differ

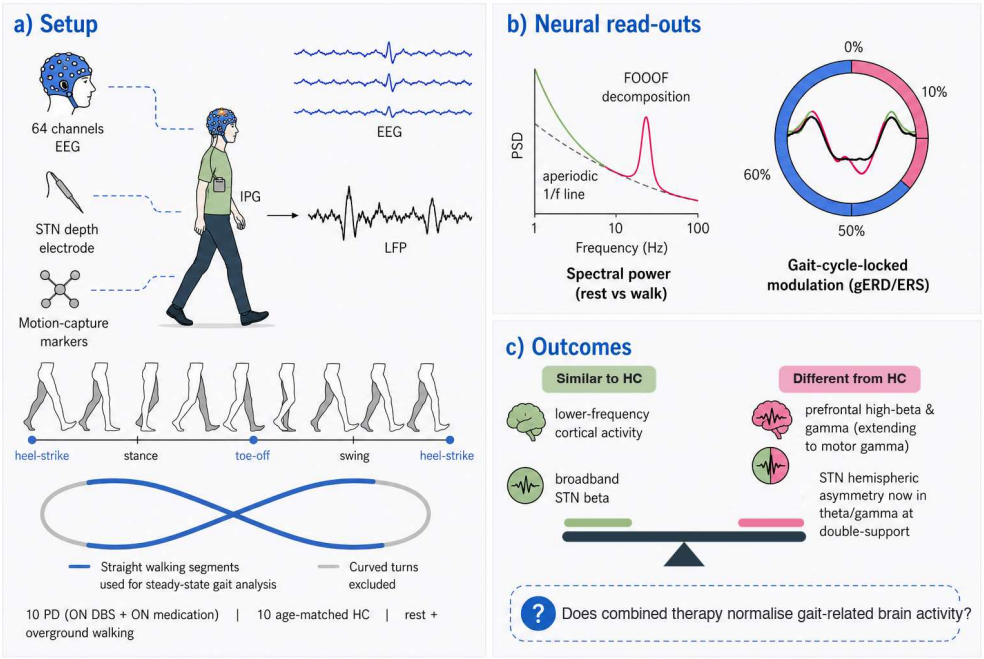
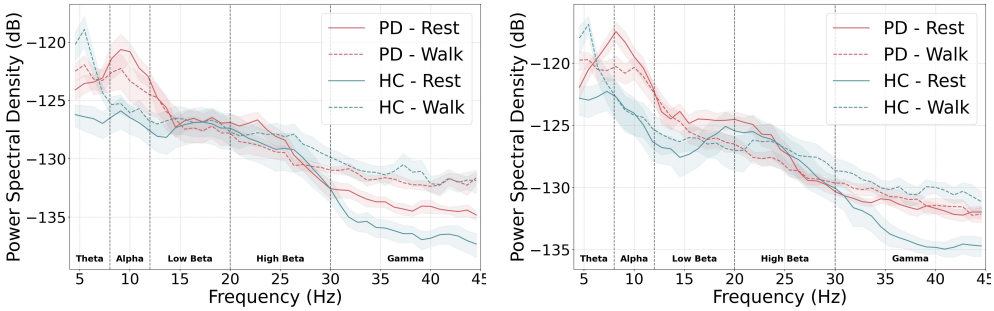


Fig. 1: **Study design and analytical framework. (a)** Setup: simultaneous 64-channel mobile EEG (both cohorts), subthalamic local field potentials via the DBS electrode (STN-LFP; PD only), and full-body motion capture during a seated resting baseline and overground walking (10 people with PD ON DBS and dopaminergic medication; 10 age-matched healthy controls, HC), with gait events from the kinematics. **(b)** Neural read-outs. Left: spectral power at rest versus walking (green, power spectral density; grey dashed, aperiodic 1/f fit; red, periodic peak), parameterised into aperiodic and periodic components with the FOOOF ("fitting-oscillations-and-one-over-f") algorithm. Right: gait-cycle-locked modulation (gait-event-related de/synchronisation, gERD/ERS); the ring represents one gait cycle running clockwise from right heel strike (0%), with double-support phases (0–10%, 50–60%) in pink and swing phases in blue, and the inset traces are schematic band-power time courses across the same cycle, drawn left to right from 0 to 100%. **(c)** Outcomes, contrasting features that were similar to HC (left) with those that differed from HC (right): overall spectral characteristics were largely preserved (two of 24 between-cohort comparisons survived FDR correction; Tab. 1), whereas residual differences persisted in prefrontal high-beta and gamma (extending to motor gamma) and in the hemispheric organisation of subthalamic gait encoding (theta and gamma, around double support).

significantly between PD and HC or between rest and walking in either the prefrontal or motor cortex (Supplementary Tab. S2).



(a) Motor cortex

(b) Prefrontal cortex

Fig. 2: **Cortical EEG spectra show alpha and beta desynchronisation during walking in both cohorts.** Median spectral power (decibels, dB; 4–45 Hz) for **(a)** motor and **(b)** prefrontal cortex, in PD (red) and HC (blue), at rest (solid lines) and during walking (dashed lines). Shaded regions, standard error of the median; vertical dashed lines, frequency-band limits (theta, alpha, beta, gamma).

Both cohorts showed significant rest-versus-walking differences in cortical periodic power, although the affected beta sub-bands differed (Tab. 2). In the motor cortex, PD showed a significant walking-related power reduction in alpha ($p_{\mathrm{FDR}} = 0.015$) and high-beta ($p_{\mathrm{FDR}} = 0.026$), whereas low-beta power did not change significantly ($p_{\mathrm{FDR}} = 0.513$). HC showed a significant power reduction in low-beta ($p_{\mathrm{FDR}} = 0.015$). In the prefrontal cortex, PD showed significant power reductions in alpha and high-beta (both $p_{\mathrm{FDR}} = 0.032$), whereas HC showed significant power reductions in alpha ($p_{\mathrm{FDR}} = 0.043$) and low-beta ($p_{\mathrm{FDR}} = 0.032$). Gamma was not included in the FOOOF parameterisation (peaks were extracted for alpha and beta only; see Methods), so the apparently larger walking-related gamma increase in HC than in PD over the motor cortex (Fig. 2a) was not tested at the PSD level; gamma cohort differences were instead assessed in the gait-phase-resolved analysis below.

Overall STN spectral activity does not differ between rest and walking

STN-LFP PSDs during rest and walking are shown in Fig. 3. Aperiodic exponent and offset did not differ significantly between conditions (Supplementary Tab. S2). Likewise, no significant rest-versus-walking differences were observed in alpha, low-beta, or high-beta peak power or centre frequency (Supplementary Tab. S3); the visually higher walking spectrum around the high-beta/gamma border (Fig. 3) corresponded to a non-significant trend in high-beta peak power (Wilcoxon signed-rank test, $p = 0.063$, $p_{\mathrm{FDR}} = 0.50$). Thus, no significant rest-versus-walking difference was detected in the analysed STN spectral parameters.

Table 1: **Two between-cohort PSD differences survive FDR correction: higher prefrontal alpha power in PD during walking and lower motor high-beta centre frequency in PD at rest.** Cortical between-cohort comparisons (PD vs. HC) of periodic parameters (Power and Centre Frequency, CF) in prefrontal and motor regions of interest (ROIs), with the beta band split into low-beta (12–20 Hz) and high-beta (20–30 Hz). Test choice is Welch's T-test or Mann-Whitney U-test depending on normality. Diff is the mean difference (PD − HC) for Welch rows and the median difference for Mann-Whitney rows. p_{FDR} uses Benjamini–Hochberg correction within each (ROI, periodic-vs-aperiodic) family. α denotes the alpha band, and low/high β the beta sub-bands given above. Significance markers: $^{*}p \leq 0.05$, $^{**}p \leq 0.01$, $^{***}p \leq 0.001$.

ROI	Condition	Parameter	Test Used	Stat	Diff	p_{raw}	p_{FDR}
Prefrontal	Rest	Alpha Power	Mann-Whitney	59.5	0.265	0.495	0.641
		Alpha CF	Welch T-Test	-0.38	-0.171	0.715	0.715
		Low Beta Power	Mann-Whitney	29.5	-0.306	0.118	0.471
		Low Beta CF	Welch T-Test	-1.10	-0.982	0.303	0.606
		High Beta Power	Welch T-Test	-0.41	-0.043	0.686	0.715
		High Beta CF	Welch T-Test	-2.32	-2.287	0.044*	0.310
	Walk	Alpha Power	Mann-Whitney	87.0	0.370	0.003**	0.035*
		Alpha CF	Not applicable	-	-	-	-
		Low Beta Power	Mann-Whitney	56.0	0.000	0.585	0.682
		Low Beta CF	Not applicable	-	-	-	-
		High Beta Power	Mann-Whitney	39.0	-0.161	0.396	0.617
		High Beta CF	Welch T-Test	-1.15	-2.108	0.286	0.606
Motor	Rest	Alpha Power	Mann-Whitney	73.0	0.267	0.088°	0.212
		Alpha CF	Welch T-Test	0.40	0.173	0.693	0.970
		Low Beta Power	Mann-Whitney	19.5	-0.568	0.022*	0.129
		Low Beta CF	Welch T-Test	-0.82	-1.146	0.451	0.774
		High Beta Power	Welch T-Test	0.13	0.017	0.897	0.980
		High Beta CF	Welch T-Test	-4.85	-4.474	< 0.001***	0.004**
	Walk	Alpha Power	Mann-Whitney	71.5	0.064	0.050°	0.200
		Alpha CF	Not applicable	-	-	-	-
		Low Beta Power	Mann-Whitney	48.0	0.000	0.898	0.980
		Low Beta CF	Welch T-Test	0.37	0.791	0.727	0.970
		High Beta Power	Mann-Whitney	28.0	-0.161	0.067°	0.200
		High Beta CF	Not applicable	-	-	-	-

Note: ° indicates $0.05 < p \leq 0.1$; * indicates $p \leq 0.05$; ** indicates $p \leq 0.01$; *** indicates $p \leq 0.001$.

Cortical gait-phase modulation differs between PD and HC

Cortical gERSPs (computed with a Morlet wavelet transform and epoched to time-warped gait cycles; see Methods) showed pronounced gait-cycle-locked modulation in both cohorts (Fig. 4a). Baseline-normalised cortical gERD/ERS was analysed using Cohort, Region, and GaitPhase (Tab. 3). This analysis revealed significant main effects of Region and GaitPhase across all five frequency bands (all $p < 0.001$). A main effect of Cohort was significant in high-beta ($F_{1,20} = 5.81$, $p = 0.026$) and gamma ($F_{1,20} = 8.77$, $p = 0.008$), but not in theta, alpha, or low-beta.

Table 2: **Both cohorts show movement-related cortical desynchronisation during walking, but in different beta sub-bands: high-beta in PD, low-beta in HC.** Cortical within-cohort rest vs. walk comparisons of periodic Power and Centre Frequency (CF) in prefrontal and motor regions of interest (ROIs), with the beta band split into low-beta (12–20 Hz) and high-beta (20–30 Hz). Mean Diff is the mean paired difference (Rest − Walk); positive values indicate Power at Rest > Power during walking (desynchronisation). α denotes the alpha band, and low/high β the beta sub-bands given above. Significance markers: $^{*}p \leq 0.05$, $^{**}p \leq 0.01$, $^{***}p \leq 0.001$. "Not applicable" rows: cases where no detectable spectral peak permitted a centre-frequency estimate.

ROI	Cohort	Parameter	Test Used	Stat	Mean Diff	p_{raw}	p_{FDR}
Prefrontal	**PD**	Alpha Power	Paired T-Test	3.56	0.154	0.006**	0.032*
		Alpha CF	Paired T-Test	-0.75	-0.469	0.479	0.719
		Low Beta Power	Paired T-Test	0.81	0.046	0.441	0.719
		Low Beta CF	Not applicable	-	-	-	-
		High Beta Power	Paired T-Test	4.04	0.228	0.003**	0.032*
		High Beta CF	Paired T-Test	-0.48	-0.575	0.661	0.793
	HC	Alpha Power	Paired T-Test	3.03	0.376	0.014*	0.043*
		Alpha CF	Not applicable	-	-	-	-
		Low Beta Power	Paired T-Test	3.38	0.289	0.008**	0.032*
		Low Beta CF	Not applicable	-	-	-	-
		High Beta Power	Paired T-Test	1.65	0.179	0.133	0.319
		High Beta CF	Paired T-Test	-0.96	-1.796	0.409	0.719
Motor	**PD**	Alpha Power	Paired T-Test	4.51	0.340	0.0015**	0.015*
		Alpha CF	Paired T-Test	0.76	0.579	0.492	0.538
		Low Beta Power	Paired T-Test	0.95	0.085	0.366	0.513
		Low Beta CF	Paired T-Test	-1.50	-1.069	0.271	0.513
		High Beta Power	Paired T-Test	3.61	0.316	0.006**	0.026*
		High Beta CF	Not applicable	-	-	-	-
	HC	Alpha Power	Paired T-Test	2.37	0.348	0.042*	0.148
		Alpha CF	Not applicable	-	-	-	-
		Low Beta Power	Paired T-Test	4.27	0.367	0.002**	0.015*
		Low Beta CF	Paired T-Test	1.14	1.984	0.335	0.513
		High Beta Power	Paired T-Test	1.80	0.173	0.105	0.294
		High Beta CF	Paired T-Test	1.17	1.042	0.307	0.513

Note: $^{\circ}$ indicates $0.05 < p \leq 0.1$; * indicates $p \leq 0.05$; ** indicates $p \leq 0.01$; *** indicates $p \leq 0.001$.

Cohort × Region interactions were significant across all frequency bands (theta: $F_{1,12859} = 51.99$, $p < 0.001$; alpha: $F_{1,12859} = 4.61$, $p = 0.032$; low-beta: $F_{1,12859} = 40.47$, $p < 0.001$; high-beta: $F_{1,12859} = 60.31$, $p < 0.001$; gamma: $p < 0.001$; Tab. 3). Post-hoc comparisons showed significant PD-vs-HC differences in the prefrontal cortex in high-beta ($t(22.3) = 2.59$, $p = 0.017$) and gamma ($t(22.3) = 3.49$, $p = 0.002$). In the motor cortex, the cohort difference was significant in gamma ($t(22.3) = 2.13$, $p = 0.045$) and marginal in high-beta ($t(22.3) = 1.98$, $p = 0.061$; Supplementary Tab. S4).

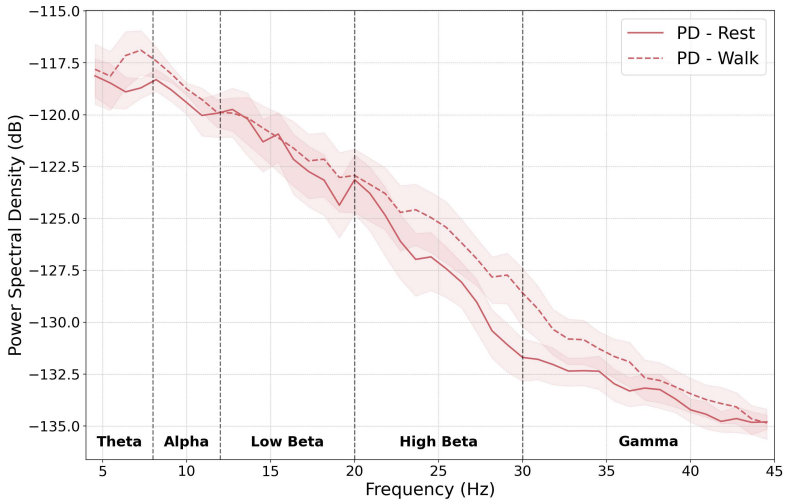
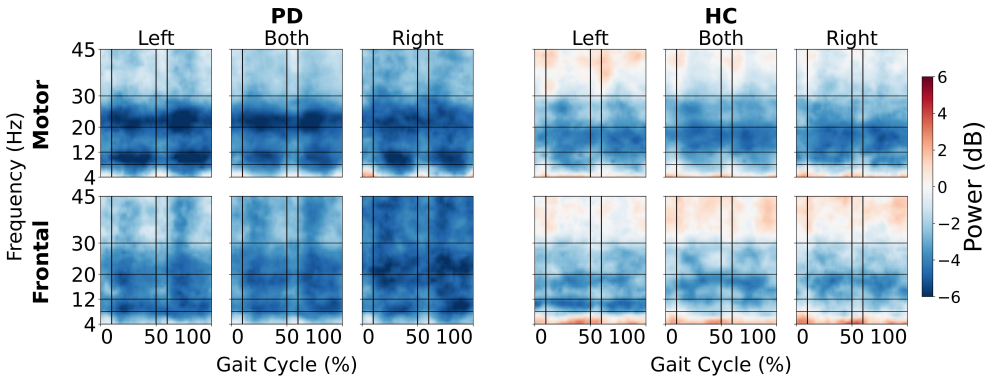


Fig. 3: **Subthalamic nucleus (STN-LFP) spectra do not differ between rest and walking under combined therapy.** Median spectral power (dB, 4–45 Hz) at rest (solid line) and during walking (dashed line) in the PD cohort. Shaded regions, standard error of the median; vertical dashed lines, frequency-band limits. Spectra are pooled across the recorded hemispheres (each subject's STN contralateral to the more clinically affected body side; see Methods).

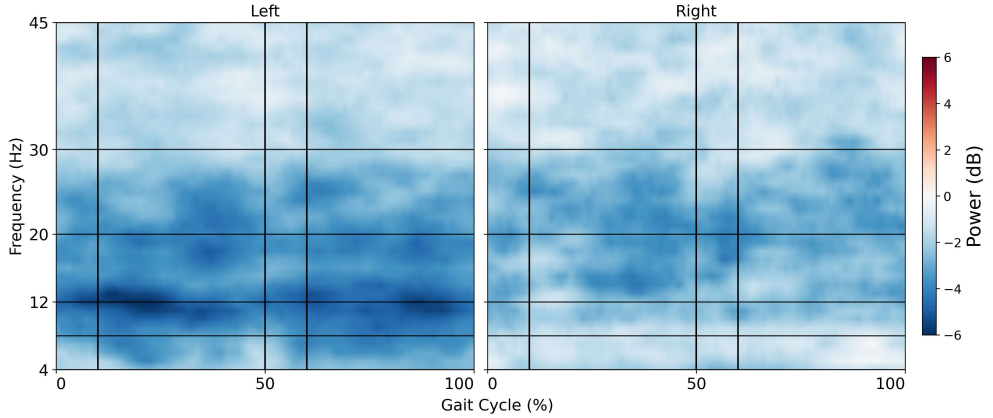
Cohort × GaitPhase interactions were also significant across all five bands (theta: $F_{3,12859} = 46.13$, $p < 0.001$; alpha: $F_{3,12859} = 12.26$, $p < 0.001$; low-beta: $F_{3,12859} = 13.63$, $p < 0.001$; high-beta: $F_{3,12859} = 4.00$, $p = 0.007$; gamma: $F_{3,12859} = 9.17$, $p < 0.001$). Post-hoc PD-vs-HC contrasts were significant during all four gait phases in gamma and during three of four gait phases in high-beta (Supplementary Tab. S4).

The time-resolved cortical profiles are shown in Fig. 5 and Supplementary Fig. S1, illustrating the temporal modulation across the gait cycle in both cohorts.

To test whether the cortical cohort differences were robust to the choice of normalisation, the data were additionally normalised to the average gait cycle rather than to the resting baseline (resting-baseline versus average-gait-cycle normalisation; see Methods; Supplementary Fig. S2). GaitPhase remained significant across all five bands, while Region was significant in low-beta ($p = 0.046$), high-beta ($p < 0.001$), and gamma ($p < 0.001$; Supplementary Tab. S5). Cohort × GaitPhase interactions remained significant in all five bands, whereas Cohort × Region interactions were no longer significant. The Cohort main effect was nominally significant only in low-beta ($p = 0.017$). Because average-gait-cycle normalisation subtracts each participant's own mean, it removes between-subject differences by construction; the overall cohort test is therefore unreliable under this normalisation, and we do not interpret this effect. Cohort main effects in theta ($p = 0.065$) and alpha ($p = 0.058$) were marginal. Post-hoc Cohort × GaitPhase contrasts showed significant PD-vs-HC differences predominantly during the double-support phases across multiple bands (Supplementary Tab. S6).



(a) **Cortical gERSPs reveal robust gait-cycle-locked spectral modulation in both cohorts, with band-specific differences between PD and HC.** Group-median cortical gERSPs across one normalised gait cycle; PD ($N = 10$) on the left, HC ($N = 10$) on the right. Within each cohort, columns show the left-hemisphere channels of each ROI (Left: C1, C3 for motor; AF3, F1 for prefrontal), all ROI channels including the midline (Both), and the right-hemisphere channels (Right: C2, C4; AF4, F2); Left and Right thus refer to EEG hemispheres, not to the recorded STN. Gait cycles are aligned to the right heel strike (0%).



(b) **Subcortical gERSPs show hemispheric differences in gait-cycle-locked STN-LFP modulation under combined therapy.** Group-median STN-LFP gERSPs in the PD cohort; right STN for $N = 6$ participants and left STN for $N = 4$ participants (one hemisphere recorded per subject from the symptom-dominant side).

Fig. 4: **Baseline-normalised cortical and subcortical gERSPs across the gait cycle. (a)** Cortical and **(b)** subcortical gERSPs, normalised to the resting baseline (dB) and time-aligned to the right heel strike, with frequency bands stacked vertically (computational details in Methods).

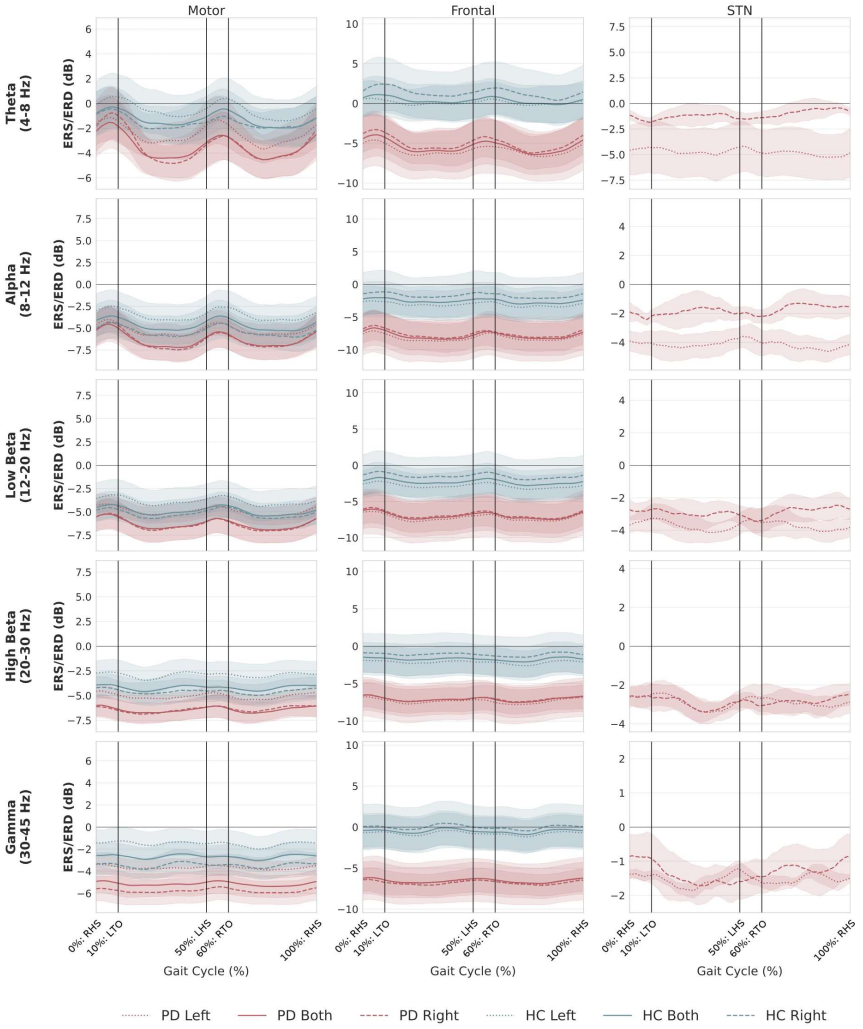


Fig. 5: **Band-resolved gait-cycle-locked gERD/ERS profiles show phase-localised cohort and hemisphere differences in higher frequency bands.** Mean gERD/ERS extracted from the baseline-normalised gERSPs in Fig. 4a and Fig. 4b (EEG averaged across channels within each ROI before group aggregation), by frequency band across the gait cycle. Cortical traces compare PD ($N = 10$) and HC ($N = 10$); subcortical traces compare right ($N = 6$) and left ($N = 4$) STN in PD. Cortical Left/Both/Right traces use the channel subsets defined in Fig. 4a; for the STN, Left/Right is the recorded hemisphere. The gait cycle is aligned to the right heel strike (RHS, 0%); LTO, LHS, and RTO mark left toe-off, left heel strike, and right toe-off. Y-axis ranges differ between panels: limits are set per frequency band so that the within-band modulation and its spread remain readable; amplitudes are therefore not comparable across panels.

Table 3: **Cortical baseline-normalised linear mixed-effects model (LMM): Cohort-by-Region and Cohort-by-GaitPhase interactions are significant in every band, while the Cohort main effect reaches significance only in high-beta and gamma.** Type III ANOVA results from the LMM on cortical baseline-normalised gait-event-related de-/synchronisation (gERD/ERS) extracted from gERSPs shown in Fig. 4 and Fig. 5. Model: `gERD/ERS ~ Cohort * Region + Cohort * GaitPhase + (1|SubjectID) + (1|GaitCycle:SubjectID)`.

Variable	Theta	Alpha	Low-Beta	High-Beta	Gamma
Cohort	df = 1, 20 F = 2.48 p = 0.131	df = 1, 20 F = 0.60 p = 0.446	df = 1, 20 F = 0.79 p = 0.384	df = 1, 20 F = 5.81 p = 0.026*	df = 1, 20 F = 8.77 p = 0.008**
Region	df = 1, 12859 F = 129.07 p < 0.001***	df = 1, 12859 F = 18.21 p < 0.001***	df = 1, 12859 F = 322.79 p < 0.001***	df = 1, 12859 F = 294.81 p < 0.001***	df = 1, 12859 F = 17.37 p < 0.001***
GaitPhase	df = 3, 12859 F = 456.66 p < 0.001***	df = 3, 12859 F = 199.34 p < 0.001***	df = 3, 12859 F = 142.88 p < 0.001***	df = 3, 12859 F = 49.74 p < 0.001***	df = 3, 12859 F = 53.38 p < 0.001***
Cohort × Region	df = 1, 12859 F = 51.99 p < 0.001***	df = 1, 12859 F = 4.61 p = 0.032*	df = 1, 12859 F = 40.47 p < 0.001***	df = 1, 12859 F = 60.31 p < 0.001***	df = 1, 12859 F = 392.79 p < 0.001***
Cohort × GaitPhase	df = 3, 12859 F = 46.13 p < 0.001***	df = 3, 12859 F = 12.26 p < 0.001***	df = 3, 12859 F = 13.63 p < 0.001***	df = 3, 12859 F = 4.00 p = 0.007**	df = 3, 12859 F = 9.17 p < 0.001***

Note: ° indicates $0.05 < p \leq 0.1$; * indicates $p \leq 0.05$; ** indicates $p \leq 0.01$; *** indicates $p \leq 0.001$.

STN activity is modulated across the gait cycle under combined therapy

Baseline-normalised STN gERD/ERS was analysed using anatomical Hemisphere and GaitPhase (Fig. 4b; Tab. 4). A significant main effect of GaitPhase was observed in low-beta ($F_{3,3632} = 3.13, p = 0.025$), high-beta ($F_{3,3632} = 2.91, p = 0.033$), and gamma ($F_{3,3632} = 3.81$, $p = 0.010$) , but not in theta or alpha. A main effect of Hemisphere was observed in alpha ($F_{1,8} = 6.47$, $p = 0.035$), reflecting deeper walking-related alpha desynchronisation in the left-STN subgroup, but in no other band. Because Hemisphere is a between-subject factor in this design (one STN per participant; $N = 4$ left vs. $N = 6$ right), this offset-type effect cannot be assessed under average-gait-cycle normalisation, which removes between-subject offsets by construction, and we do not interpret it further.

Hemisphere × GaitPhase interactions were significant in theta ($F_{3,3632} = 4.63$, $p = 0.003$) and gamma ($F_{3,3632} = 4.57$, $p = 0.003$). No significant interactions were

observed in alpha ($p = 0.192$), low-beta ($p = 0.792$), or high-beta ($p = 0.679$). Post-hoc Left-vs-Right comparisons did not reach significance within any individual gait phase after correction for multiple comparisons (Supplementary Tab. S7).

Table 4: **STN baseline-normalised linear mixed-effects model (LMM): significant Hemisphere-by-GaitPhase interactions in theta and gamma, and a Hemisphere main effect in alpha.** Type III ANOVA results from the LMM on baseline-normalised STN-LFP gERD/ERS extracted from gERSPs shown in Fig. 4b. Model: `gERD/ERS ~ Hemisphere * GaitPhase + (1|SubjectID)`.

Variable	Theta	Alpha	Low-Beta	High-Beta	Gamma
Hemisphere	df = 1, 8 F = 2.44 p = 0.157	df = 1, 8 F = 6.47 p = 0.035*	df = 1, 8 F = 1.22 p = 0.301	df = 1, 8 F = 0.19 p = 0.671	df = 1, 8 F = 0.05 p = 0.830
GaitPhase	df = 3, 3632 F = 0.51 p = 0.674	df = 3, 3632 F = 0.53 p = 0.659	df = 3, 3632 F = 3.13 p = 0.025*	df = 3, 3632 F = 2.91 p = 0.033*	df = 3, 3632 F = 3.81 p = 0.010**
Hemisphere × GaitPhase	df = 3, 3632 F = 4.63 p = 0.003**	df = 3, 3632 F = 1.58 p = 0.192	df = 3, 3632 F = 0.35 p = 0.792	df = 3, 3632 F = 0.51 p = 0.679	df = 3, 3632 F = 4.57 p = 0.003**

Note: ° indicates $0.05 < p \leq 0.1$; * indicates $p \leq 0.05$; ** indicates $p \leq 0.01$; *** indicates $p \leq 0.001$.

Average-gait-cycle normalisation and stepping-limb alignment confirm STN gait-phase and hemispheric effects

To check whether the STN gait-phase and hemispheric effects were robust to key analytical choices, we repeated them under two variations: an alternative normalisation (average gait cycle instead of the resting baseline) and an alternative alignment of the gait cycle (relative to the stepping limb instead of anatomical side; see Methods). With average-gait-cycle normalisation, the main effect of GaitPhase was significant in low-beta ($p = 0.018$), high-beta ($p = 0.007$), and gamma ($p = 0.009$; Supplementary Tab. S8). Hemisphere × GaitPhase interactions were again significant in theta ($p = 0.006$) and gamma ($p = 0.005$), but in no other band. Post-hoc comparisons showed significant Left-vs-Right differences in theta during both double-support phases (IDS: $p = 0.027$; FDS: $p = 0.039$) and during RLS ($p = 0.033$), and in gamma during IDS ($p = 0.009$) and FDS ($p = 0.029$; Supplementary Tab. S9).

To assess STN modulation relative to the stepping limb, an additional analysis aligned each STN recording to the ipsilateral heel strike (Supplementary Fig. S3). For baseline-normalised data, Hemisphere × GaitPhase interactions were significant in theta ($p = 0.020$) and gamma ($p = 0.021$), but not in alpha, low-beta, or high-beta (Supplementary Tab. S10). With average-gait-cycle normalisation, these interactions

remained significant in theta ($p = 0.030$) and gamma ($p = 0.019$; Supplementary Tab. S12).

Post-hoc gait-phase contrasts reached significance only with average-gait-cycle normalisation. Differences were observed in theta during the double-support phase following the contralateral heel strike (FDS: $t(111) = 2.61$, $p = 0.010$) and in gamma during the double-support phase following the ipsilateral heel strike (IDS: $t(111) = -2.24$, $p = 0.027$; Supplementary Tabs. S11 and S13).

Discussion

This study investigated cortical and subthalamic activity during gait in PD under ongoing STN-DBS and dopaminergic therapy. To our knowledge, it is the first to characterise gait-phase-resolved cortical and subthalamic activity in people with PD under their ongoing combined STN-DBS and dopaminergic therapy and to compare the cortical dynamics directly with age-matched HC. Overall spectral activity showed relatively few differences from HC, limited to higher prefrontal alpha power during walking and a lower motor high-beta centre frequency, whereas resolving neural activity across the gait cycle revealed persistent differences in its temporal organisation. Cortically, these differences were most pronounced in high-beta and gamma activity, particularly in prefrontal regions. In the STN, activity was modulated across the gait cycle in low-beta, high-beta, and gamma despite the absence of significant rest-versus-walking differences in the analysed spectral features. Gait-phase-dependent hemispheric modulation was additionally evident in theta and gamma. Together, these findings indicate that relatively similar overall spectral activity under combined therapy can coexist with altered temporal organisation of cortical and subthalamic oscillations across the gait cycle.

Despite relatively similar overall spectral activity between PD and HC, residual differences were evident in the spectral organisation and gait-related modulation of cortical activity. Aperiodic spectral parameters did not differ between cohorts, while periodic activity showed higher prefrontal alpha power during walking and a lower motor high-beta centre frequency in PD. Higher alpha power is conventionally interpreted as reduced cortical activation or functional inhibition of the underlying region rather than stronger engagement [15, 30, 31]; the higher prefrontal alpha power during walking in PD is therefore more consistent with a relatively reduced prefrontal engagement during steady-state walking than with increased prefrontal recruitment. In addition, walking was associated predominantly with high-beta ERD in PD but low-beta ERD in HC. Movement-related alpha and beta desynchronisation is a well-established feature of cortical motor activity [15, 21, 32], while both dopaminergic treatment and DBS can modify cortical beta oscillations in PD [7–10]. The present results suggest that, even when the magnitude of beta activity is relatively similar between cohorts, its spectral organisation remains altered. This distinction is relevant because beta peak frequency can vary with dopaminergic state independently of consistent changes in beta power [33]. The lower motor high-beta centre frequency and different beta sub-band showing significant gait-related desynchronisation therefore point towards a residual reorganisation of cortical beta activity that is not captured by beta power alone.

More pronounced cohort differences emerged when cortical activity was resolved across the gait cycle. Both PD and HC showed robust gait-phase modulation across frequency bands, consistent with the rhythmic modulation of cortical oscillations during walking reported in healthy participants [18, 19]. However, the temporal profiles of this modulation differed between cohorts across all analysed bands. Previous mobile EEG studies have similarly demonstrated that cortical abnormalities in PD vary over the gait cycle rather than being expressed solely as differences in average activity [22]. The present findings extend this work by showing that such differences remain evident in participants receiving combined STN-DBS and dopaminergic therapy.

The strongest residual cortical differences under baseline normalisation were found in high-beta and gamma activity, particularly in prefrontal regions, with an additional gamma difference over motor cortex. Altered cortical recruitment during gait in PD has previously been reported across motor and prefrontal regions [34–36]. The prominence of prefrontal differences in the present study is consistent with evidence for increased involvement of higher-order cortical regions in gait control in PD [36]. Importantly, our findings further identify high-beta and gamma as the frequencies in which these residual differences were most consistently expressed under combined therapy.

Gamma activity is particularly relevant in this context because cortical gamma modulation has been associated with lower-limb movement and specific phases of the gait cycle [21, 37]. In the present study, PD–HC differences in gamma were evident across all four analysed gait phases, while high-beta differences were present across three phases, with the remaining phase showing a similar trend. The differences therefore did not reflect a single isolated gait event but persisted across much of the gait cycle. Together with the altered time-resolved profiles, this suggests that the timing and magnitude of cortical high-frequency recruitment during walking differ between PD and HC. This extends previous observations of altered gait-phase-dependent cortical activity in PD [22] by identifying high-beta and gamma dynamics as prominent residual features during combined STN-DBS and dopaminergic treatment.

The cohort-by-gait-phase effects were comparatively robust to the choice of normalisation, whereas differences between the prefrontal and motor regions were more sensitive to it. Thus, altered temporal modulation across the gait cycle appears to be a robust feature of the PD–HC difference, whereas the regional (prefrontal-versus-motor) differences partly reflect sustained walking-state activity relative to rest—a constant engagement across the gait cycle that baseline normalisation retains and average-gait-cycle normalisation removes by construction. They are therefore best interpreted as differences in overall cortical engagement during walking rather than within-cycle modulation.

A similar distinction between overall spectral activity and within-cycle dynamics emerged in the STN. Although no significant rest-versus-walking differences were detected in aperiodic parameters or alpha and beta peak characteristics, STN activity was significantly modulated across gait phases in low-beta, high-beta, and gamma. Thus, the absence of a detectable change between rest and walking did not imply an absence of gait-related STN dynamics; rather, averaging activity across the walking period obscured temporal modulation occurring within individual gait cycles.

Phase-dependent STN oscillations during walking have been demonstrated in several previous studies [4, 27, 38, 39]. Louie et al., for example, took a data-driven, machine-learning approach, identifying patient-specific spectral biomarkers that classified individual gait events from cortico-subthalamic recordings in three people with PD without marked gait impairment [39]. Together, these studies establish that STN oscillatory activity carries temporally structured information about individual steps. Whereas that work derived individualised, data-driven gait-event decoders, the present study used a hypothesis-driven, group-level characterisation of STN gait dynamics under combined therapy, alongside cortical comparisons with age-matched HC. Importantly, this within-cycle organisation remained detectable under the clinically relevant combination of STN-DBS and dopaminergic therapy, even when changes in overall spectral activity between rest and walking were limited.

This interpretation is further supported by recent findings from Scafa et al., who showed that STN spectral activity continues to encode locomotor states under standard-of-care L-DOPA and STN-DBS, although the dynamic range of this encoding is markedly reduced [29]. In particular, they reported that activity-dependent high-beta and gamma modulation persisted, albeit attenuated, under combined therapy, whereas low-beta modulation lacked reproducible patterns across participants [29]. While Scafa et al. examined transitions between locomotor states such as sitting, standing, and walking, the present gait-event-locked analysis resolves neural dynamics within walking itself. Together, these findings indicate that treatment does not eliminate the temporal organisation of STN activity related to locomotion, but that relevant information may be expressed in transient and behaviourally structured modulations rather than in the average power spectral level during walking.

Beyond the presence of within-cycle modulation, gait-phase-dependent organisation was also reflected in the hemispheric STN effects. Previous studies have demonstrated alternating and lateralised STN activity during stepping [4, 26, 38, 39]. Fischer et al., for example, reported stepping-foot-locked beta modulation that alternated reciprocally between the left and right subthalamic nuclei across the stepping cycle [38]. In the present cohort under combined STN-DBS and dopaminergic therapy, Hemisphere $\times$ GaitPhase interactions were most consistently detected in theta and gamma and remained evident when activity was aligned relative to the stepping limb. Although the precise phase-localised differences varied with normalisation, the converging interaction effects support the persistence of gait-phase-dependent hemispheric organisation of STN activity under combined therapy.

The distinction between overall spectral activity and gait-phase-dependent dynamics has important implications for the development of gait-related biomarkers. STN beta activity is strongly associated with the parkinsonian motor state, is reduced by dopaminergic treatment and DBS, and has become a principal control signal for adaptive DBS [5, 12, 40]. Gait, however, is an inherently cyclic behaviour that requires neural activity to be coordinated continuously with alternating periods of stance, swing, and weight transfer. Consequently, a spectral feature that distinguishes clinical motor states when averaged over seconds may not capture the neural dynamics most relevant to individual phases of walking.

Evidence from intracranial recordings increasingly supports this distinction. Gait phase and gait events can be decoded from phase-dependent cortical and STN spectral activity [4, 39], and Scafa et al. recently demonstrated that ongoing locomotor activities can be decoded from STN dynamics across different treatment conditions [29]. Importantly, their activity-dependent DBS framework used this locomotor information to adapt stimulation according to behavioural context and improved locomotor deficits in a proof-of-concept study [29]. Complementing this STN-based approach, Louie et al. identified patient-specific gait-phase biomarkers from pallidal and cortical field potentials and used them to deliver gait-synchronised adaptive DBS, which reduced gait variability and falls in a randomised feasibility trial [41]. Both frameworks rely on individualised, data-driven biomarker discovery within the treated motor circuit to steer closed-loop therapy, whereas the present study uses an a priori, group-level comparison with age-matched HC to characterise which gait-phase-resolved features remain altered under combined therapy and could serve as candidate targets for such strategies. Because these candidate features are physiologically interpretable, this approach also offers an alternative to purely data-driven target selection, providing transparency and control over which signals are modulated—an advantage for closed-loop applications. These developments suggest that gait-specific neuromodulation may benefit from neural markers that complement the beta signals traditionally used to track the general parkinsonian motor state. Exploiting such gait-phase-resolved markers in closed-loop systems would, however, require sensing and control at the temporal resolution of individual gait phases, i.e. well below one second, rather than the seconds-scale averaging used for beta-based adaptive DBS.

The present findings identify two potentially relevant sources of such information. First, residual cortical differences under combined treatment were concentrated in gait-phase-dependent high-beta and gamma activity, particularly over prefrontal regions. Second, STN activity retained substantial within-cycle modulation even when overall rest-versus-walking spectral differences were limited. These findings do not establish high-beta, gamma, or individual gait-phase effects as biomarkers of gait impairment, but they narrow the candidate signal space towards neural features that preserve the temporal structure of walking. An important next step will therefore be to determine whether these dynamics are associated with quantitative gait impairment and whether incorporating gait-phase information improves the detection of impaired walking beyond measures based on average spectral magnitude alone.

Several limitations constrain the interpretation of these findings. All PD recordings were obtained in the ON-medication and ON-DBS state, and no OFF-treatment condition was recorded. This state was chosen deliberately because it is the clinically relevant one in which gait impairment persists despite individually optimised STN-DBS and dopaminergic therapy, but the design does not separate treatment effects from disease-related differences; differences from HC are therefore described as residual differences under treatment rather than as evidence of residual pathology or incomplete normalisation. The sample was modest, with ten participants per cohort and STN recordings further split into four left- and six right-hemisphere recordings, limiting sensitivity to smaller cohort and hemispheric effects. The PD cohort spanned mild to moderately severe motor impairment (total UPDRS-III 8–45, gait item 1–3;

Tab. 5), and with ten participants the influence of impairment severity on the observed dynamics could not be examined.

STN-LFPs were recorded from a single hemisphere per participant, deliberately chosen as the STN contralateral to the more clinically affected body side (defined per participant from the UPDRS-III lateralised motor score) so that the recording reflected the hemisphere most closely associated with each participant's motor impairment. Although the Percept^{TM} PC supports bilateral sensing during ongoing stimulation, recording this single, clinically defined hemisphere means that hemisphere comparisons are between participants rather than bilateral within-subject comparisons, which limits the interpretation of lateralised STN dynamics. In addition, the turning segments of the figure-of-eight walking path were excluded because of constraints of the motion-capture setup, restricting the present analyses to straight walking. Future bilateral recordings and paradigms incorporating turning and other challenging gait conditions could determine whether the observed temporal dynamics generalise to gait situations in which PD-related impairments are more pronounced.

Finally, mobile EEG during walking remains susceptible to motion and muscle artefacts. Theta-band measures warrant particular caution, as the theta band borders the 4 Hz high-pass cutoff and overlaps with harmonics of the stepping rhythm (see Methods), whereas the analysed gamma band (up to 45 Hz) lies largely below the dominant frequency range of muscle activity. Extensive preprocessing and independent-component-based artefact rejection were applied, but residual contamination, including broadband muscle activity extending into the gamma band, cannot be excluded. Some regional post-hoc effects also depended on the normalisation approach, although the cohort-by-gait-phase interactions were more consistent, reflecting the current lack of standardised normalisation procedures for gait electrophysiology [42]. Future studies should directly relate the cortical and STN dynamics identified here to quantitative gait measures such as speed, stride length, variability, and stability [22]; a companion study relates cortical and subthalamic dynamics during walking to distinct gait domains in PD [43]. Such brain–behaviour associations, ideally assessed across treatment states, will be important for determining which of the residual neural dynamics identified here are functionally linked to persistent gait impairment.

Simultaneous cortical EEG and STN-LFP recordings during overground walking reveal that gait-related neural activity in PD remains distinct from HC under combined STN-DBS and dopaminergic therapy, despite relatively limited differences in overall spectral activity. Residual cortical differences were concentrated in gait-phase-dependent high-beta and gamma activity, while STN oscillations retained within-cycle and hemispheric modulation that was not detected by rest-versus-walking spectral comparisons. These findings highlight temporal organisation as an important dimension of gait-related neural activity that is lost when oscillations are averaged across the gait cycle. Gait-specific biomarkers and neuromodulation strategies may therefore benefit from capturing when neural activity occurs within the gait cycle in addition to its overall spectral magnitude.

Methods

Participants

Ten individuals with PD (mean age ± SD = 61.7 ± 8.3 years, 3 female) with chronic bilateral STN-DBS and 10 age-matched HC (mean age ± SD = 67.4 ± 2.6 years, 5 female) were enrolled. The groups did not differ significantly in age (Welch's $t(10.7) = -2.07$, $p = 0.063$), nor in sex distribution (Fisher's exact test, $p = 0.65$). Further details can be found in Tab. 5. PD participants had been diagnosed with idiopathic, non-tremor-dominant Parkinson's disease, had undergone STN-DBS implantation at least one year before enrolment, and met at least one of two separate motor criteria: gait impairment (UPDRS-III item 3.10 ≥ 1) or postural instability (UPDRS-III item 3.12 ≥ 1). All PD participants had a fully implanted Percept^{TM} PC neurostimulator and were tested ON dopaminergic medication and ON DBS at their individually optimised therapeutic settings. Controls reported no neurological, orthopaedic, rheumatologic, psychiatric, or sensory impairments.

Table 5: **Clinical characteristics of the Parkinson's disease (PD) cohort.** Each row lists the participant identifier (PID), sex, age, Unified Parkinson's Disease Rating Scale Part III (UPDRS-III) subscores for gait (item 3.10) and postural instability (item 3.12), the total UPDRS-III score, the implanted subthalamic nucleus (STN) side, and the bipolar sensing-contact pair used for the STN-LFP recording (the active stimulation contact lies between the sensing contacts; see Methods). [a]For PID 208, the separately recorded resting baseline used pair 0–3. All PD recordings were obtained ON medication and ON DBS at the individually optimised clinical setting; detailed per-subject DBS programming parameters (amplitude, frequency, pulse width) and levodopa equivalent dose were not retrievable from the clinical records and are therefore not reported here. The STN-side column lists the anatomical side of the bipolar recording, which by inclusion criterion corresponds to the STN contralateral to the more clinically affected body side (defined per subject from the UPDRS-III lateralised motor score).

PID	Cohort	Sex	Age (yrs)	UPDRS-III Gait	Postural Instab.	Total UPDRS-III	STN side	Sensing pair
201	PD	M	65	1	2	23	L	0–2
202	PD	M	70	1	1	14	R	1–3
203	PD	F	51	1	1	10	L	1–3
204	PD	M	52	3	1	29	L	1–3
205	PD	M	53	2	1	22	R	0–2
206	PD	M	65	2	2	44	R	0–2
207	PD	F	77	3	1	45	R	0–2
208	PD	M	64	3	1	24	R	1–3[a]
209	PD	M	60	2	0	12	L	1–3
210	PD	F	60	1	0	8	R	1–3

Inclusion criteria required a Montreal Cognitive Assessment (MoCA; [44]) score $\geq$ 20; exclusion criteria were significant gait-interfering comorbidities and any contraindication to EEG or motion-capture instrumentation.

The study was approved by the Cantonal Ethics Commission Zurich (BASEC 2022-01382) and conducted in accordance with the Declaration of Helsinki and local regulations. All procedures involving human participants adhered to institutional guidelines on data protection and safety.

Study protocol

We analysed data from two experimental conditions: (i) a 2-minute eyes-open, seated resting baseline, and (ii) a 6-minute overground figure-eight walking task at a self-selected, comfortable speed along a path defined by two cones placed 10 m apart (Fig. 1A). Only the straight-walking segments between the turns were retained; turns were excluded to avoid the associated variability. EEG, STN-LFPs (PD only), and full-body motion capture were recorded continuously.

Data acquisition

Cortical activity was recorded using a 64-channel mobile EEG system (Smarting Pro X™, mBrainTrain®) at 2000 Hz with an EasyCap® 64-channel cap following the international 10-20 placement system, with electrode impedances maintained below 10 kΩ. In PD participants, STN-LFPs were recorded from the Percept™ PC BrainSense™ interface at 250 Hz, contralateral to the symptom-dominant side, using a bipolar configuration centred on the active stimulation contact (the two sensing contacts immediately above and below the active stimulation contact on the Medtronic 3389 lead); in subjects whose active stimulation contact was at the top or bottom of the lead, an adjacent non-extremity contact pair was used instead so that the bipolar pair always straddles the active contact. Whole-body kinematics were acquired at 100 Hz with a 16-camera Vicon® system using a 62-marker full-body model. EEG–Vicon synchronisation was achieved using hardware keyboard triggers visible to both systems. EEG–LFP synchronisation used a brief DBS amplitude reduction (0.5 mA) producing an artefact detectable in both modalities [45].

Signal processing

All analyses were performed in Python (v3.11.15) with MNE-Python (v1.12.1) for neural data processing. EEG preprocessing followed a multistep pipeline, outlined in Fig. 6, comprising: automated bad-channel detection (based on kurtosis, correlation, variance, and amplitude thresholds); epoch-level artefact rejection with AutoReject v0.4.3 [46]; manual channel removal of remaining noisy channels; removal of outer-ring electrodes prone to motion artefacts; zero-phase finite impulse response (FIR) 4–100 Hz band-pass filtering (windowed-sinc design, MNE-Python defaults); common-average referencing; and Infomax independent component analysis (ICA). The 4 Hz high-pass cutoff suppresses slow gait-related motion artefacts dominant below 4 Hz during overground walking; the delta band was therefore not analysed, and theta-band

measures should be interpreted with awareness of residual low-frequency contamination, particularly in STN-LFP recordings. Independent components were classified using ICLabel [47], a deep-learning classifier that probabilistically labels each component as brain or a specific non-neural source (muscle, eye, heart, line/channel noise, or other). Components classified as non-neural (probability $\geq 50\%$ in any non-brain category) were removed; components classified as "other" were reviewed manually with the same 50% probability cutoff. After ICA cleanup, signals were reconstructed onto the original channels. A before-and-after example of the pipeline for a representative participant is shown in Supplementary Fig. S4.
STN-LFPs were band-pass filtered with the same zero-phase FIR filter (4–100 Hz) to harmonise spectral content with EEG. Motion-capture data were segmented to extract straight-walking periods, and gait events (heel strikes and toe-offs) were detected using the foot-velocity method [48]. Per-subject per-condition epoch counts after preprocessing are provided in Supplementary Tab. S1, confirming that the majority of segmented epochs survived artefact rejection in both cohorts and conditions.

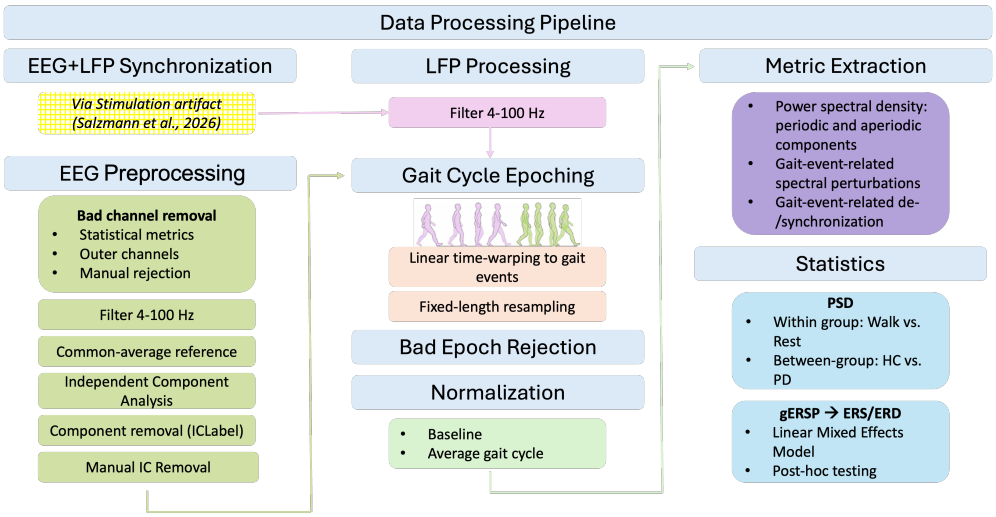


Fig. 6: **Multi-stage EEG preprocessing pipeline used to remove non-neural and motion-related artefacts from mobile gait recordings.** Preprocessing applied to each subject's continuous EEG (and, where available, STN-LFP) before spectral analysis: automated bad-channel detection, AutoReject epoch-level rejection [46], removal of motion-prone outer-ring electrodes, zero-phase 4–100 Hz band-pass filtering, common-average referencing, and Infomax ICA with ICLabel component classification (manual review of the "other" category at the 50% cutoff).

Gait cycle epoching

Continuous EEG and LFP data were segmented into gait cycles defined by right heel strike (RHS, 0%), left toe-off (LTO, 10%), left heel strike (LHS, 50%), right toe-off

(RTO, 60%), and the subsequent right heel strike (RHS, 100%). The IDS phase is defined between RHS and LTO, LLS between LTO and LHS, FDS between LHS and RTO, and RLS between RTO and the next RHS.

Each gait cycle was first linearly time-warped to these canonical phase landmarks and resampled to fixed lengths ([49], EEG: 2200 samples; STN-LFP: 275 samples; according to the average gait cycle length = 1.1 seconds). Artefactual epochs identified in either modality were removed jointly to maintain correspondence over EEG and STN-LFP recordings.

Neural metrics

Metrics were computed for two regions of interest (ROIs) that were defined a priori from the EasyCap 64-channel layout (not by any data-driven selection): the prefrontal region (EEG channels AF3, F1, Fz, F2, AF4) and the motor region (EEG channels C3, C1, Cz, C2, C4). PSDs were calculated for epoched EEG and DBS data using Welch's method (MNE-Python). The FFT length was set to the full epoch length to maximise frequency resolution for spectral parameterisation, with a Hanning window to limit spectral leakage. Analysis was restricted to 4–45 Hz. EEG channel-PSDs were averaged within ROIs, then averaged across epochs to obtain one mean PSD per subject.

For group-level visualisation, the median and the standard error of the median (computed as the median absolute deviation divided by $\sqrt{n}$) were calculated on the linear power values and then converted to decibels.

To distinguish between specific oscillatory changes and broadband spectral shifts, the power spectra were decomposed using the "Fitting Oscillations & One-Over-F" algorithm (FOOOF v1.1.1, [50, 51]). The model was fitted to the 4–45 Hz range using the fixed aperiodic mode. Peak detection was configured with a minimum peak height of 0.09 log units, a maximum of three peaks, peak width limits of 2–12 Hz, and a relative threshold of two times the standard deviation of the spectrum. Aperiodic parameters (offset and exponent) and periodic parameters (centre frequency (CF) and power) were extracted specifically for the alpha (8–12 Hz) and beta (12–30 Hz) bands. For statistical handling, if a subject exhibited no detectable peak within a specific band, the peak power for that band was imputed as zero ($\log_{10}$ power units, the native FOOOF scale). Across the analysed alpha, low-beta, and high-beta bands, this occurred in 121 of 300 subject-by-ROI-by-condition cases, affecting every participant at least once; missing peaks were most common where no clear oscillatory peak rises above the aperiodic fit.

Time–frequency representations (TFRs) were computed using Morlet wavelets with a fixed full-width half-maximum of 200 ms and a frequency-dependent number of cycles. Two different normalisations were used: baseline normalisation compared walking power to the average power of the resting baseline, whereas average-gait-cycle normalisation compared walking power to the average power across the participant's gait cycle. Both were expressed as decibel change. The analysis focused on baseline-normalised gERSPs to capture all gait-related changes, without risking blurred main effects and interactions due to excessively strong gait-phase effects. gERD/ERS curves were obtained by averaging gERSP power within each frequency band over the gait

cycle. To analyse direct limb-control activity, a supplementary analysis aligned gERSPs ipsilaterally to the gait cycle. Because the gait cycle was anchored at RHS (0%) and left heel strike (50%), right STN recordings retained their original alignment while left STN recordings were circularly shifted by –50%. This synchronised the ipsilateral heel strike to 0% and the contralateral heel strike to 50% across all recordings, yielding a complete gait cycle, defined by: ipsilateral heel strike (IHS, 0%), contralateral toe-off (CTO, 10%), contralateral heel strike (CHS, 50%), ipsilateral toe-off (ITO, 60%), and the subsequent ipsilateral heel strike (IHS, 100%). For this new alignment, the gait phases have been redefined as such: Initial double support (IDS) phase is defined between IHS and CTO, contralateral leg swing (CLS) between CTO and CHS, final double support (FDS) between CHS and ITO and ipsilateral leg swing (ILS) between ITO and the next IHS.
Analyses were performed separately for motor and prefrontal cortical regions, and, in PD, for STN-LFPs recorded from left- or right-sided electrodes. Grand medians were computed pixel-wise across all subjects to create the cohort gERSP heatmaps; the band-resolved gERD/ERS traces (Fig. 5 and Supplementary Fig. S1) instead show the across-subject mean ± standard error of the mean per gait-cycle bin.

Statistical analysis

Power spectral density

Statistical analysis was performed on the extracted FOOOF parameters to assess within-subject (rest vs. walk) and between-cohort (PD vs. HC) differences. Distributions were assessed for normality (Shapiro-Wilk); within-subject comparisons used paired t-tests or Wilcoxon signed-rank tests, and between-subject comparisons used Welch's t-test or Mann-Whitney U-tests, depending on normality. p-values were Benjamini–Hochberg FDR-corrected [52] separately for periodic (power, centre frequency) and aperiodic (offset, exponent) parameter families.

Gait-event-related spectral perturbations

Statistical analyses of cortical gERSPs across individual gait cycles were performed using linear mixed-effects models (LMM; R 4.5.2; `lme4`). Models were run separately for each frequency band, with gERD/ERS values (decibel median power per factor level) extracted from gERSPs as the dependent variable. To account for within-subject dependency and inter-individual variability, the models included random intercepts for Subject and for GaitCycle nested within Subject. Competing model structures were compared using Bayesian Information Criterion (BIC) and log-likelihood tests. Fixed-effect significance was evaluated using Type III ANOVA (`lmerTest`), with denominator degrees of freedom approximated by Satterthwaite's method; the resulting large denominator degrees of freedom reflect the many gait cycles contributing to each model. For significant interactions, post-hoc pairwise contrasts were obtained from `emmeans` and FDR-adjusted (Benjamini–Hochberg) within each emmeans family; reported post-hoc p-values are therefore FDR-corrected. The best-fitting and still

converging model for cortical gERSPs was:

$$\begin{aligned}\text{Band}_{\text{ERD/ERS}} \sim \text{Cohort} \times \text{Region} + \text{Cohort} \times \text{GaitPhase} \\ + (1 \mid \text{Subject}) + (1 \mid \text{GaitCycle} : \text{Subject}),\end{aligned}$$

where Cohort is a two-level factor (PD, HC), Region is a two-level factor (prefrontal, motor; averaged across left, right, and midline sites), and GaitPhase is a four-level factor (IDS, LLS, FDS, RLS).

In PD participants, hemispheric specificity of STN-LFP modulation was evaluated using the model:

$$\text{Band}_{\text{ERD/ERS}} \sim \text{Hemisphere} \times \text{GaitPhase} + (1 \mid \text{Subject}),$$

which tested for lateralised spectral modulation of the STN-LFP across the gait cycle, with Hemisphere as a two-level factor (Left, Right STN). Hemisphere was entered as a between-subjects fixed factor (rather than pooling left- and right-STN recordings into a single group) for two reasons: (i) STN recordings were obtained from a single bipolar Percept channel per subject, recorded contralateral to the symptom-dominant body side (see Data acquisition)), such that Hemisphere represents the anatomical side of the recorded STN (Left, Right); and (ii) the canonical gait-cycle anchor (0% = right heel-strike) maps differently onto the two anatomical sides—for the right STN it corresponds to the ipsilateral heel-strike, whereas for the left STN it corresponds to the contralateral heel-strike—so a Hemisphere × GaitPhase interaction can capture side-dependent gait-phase modulation that would be hidden by averaging across hemispheres. Unlike the cortical model, this interaction structure was not the most parsimonious by information criteria: by the Bayesian information criterion (BIC) a simpler additive model (Hemisphere + GaitPhase) was preferred in most bands, an interaction-containing structure being favoured only in theta, while by the Akaike information criterion (AIC) the ranking was mixed and the between-model differences small (Supplementary Tab. S14; anatomical and ipsi/contra alignments give identical fits). The Hemisphere × GaitPhase term was therefore retained *a priori* to test the hypothesis of phase-dependent STN lateralisation rather than on parsimony grounds, consistent with the interaction reaching significance in the theta and gamma bands; a variant adding a gait-cycle random intercept lowered AIC in theta and gamma but produced singular fits and was not adopted. The UPDRS-III score was additionally evaluated as a covariate but did not improve model fit and was therefore not retained.

Baseline-normalised and average-gait-cycle-normalised gERSPs

The baseline normalisation expresses gait-cycle power as decibels relative to the average power in a pre-walk seated window (the 2-minute eyes-open, seated resting baseline; see Study protocol), allowing both within-cycle and across-condition (rest vs. walking) comparisons of absolute power changes. The average-gait-cycle normalisation instead centres each cycle's TFR around its own subject- and channel-specific time-mean across the gait cycle, removing the slow walking-state offset and

between-subject offsets by construction so that the displayed values reflect within-cycle phase-dependent modulation. Both normalisations were analysed in parallel with identical LMM specifications. Because the average-gait-cycle normalisation removes between-subject offsets, the random-intercept variance for SubjectID is essentially zero under that normalisation (the singular-fit warning issued by lme4 reflects this designed-in property rather than a numerical instability), and the fixed-effect F-tests remain interpretable; the cohort-by-gait-phase and hemisphere-by-gait-phase interactions observed under baseline normalisation replicate under the average-gait-cycle normalisation (Tab. S5–S6 and S8–S9), supporting the robustness of the cycle-locked modulation.

Acknowledgements. The authors sincerely thank the University Hospital Zurich, the Senior:innen-Universität Zurich (UZH3), Parkinson Stiftung Schweiz, and SturzZentrum Schweiz for their support and help. This study was funded by The LOOP Zurich and the Vontobel Foundation. The funders played no role in study design, data collection, analysis and interpretation of data, or the writing of this manuscript.

Author contributions. L.S. and A.S.B. were involved in all aspects of the study and contributed equally to this work. Z.M. contributed to conceptualisation, data collection and processing of the gait data. A.F. contributed to participant recruitment and conceptualisation. W.R.T. contributed to supervision and funding acquisition. V.P. contributed to data analysis, writing, reviewing, and supervision. L.I. contributed to data analysis, writing, reviewing, and supervision. D.K.R. contributed to conceptualisation, supervision, and reviewing. O.L. and R.G. contributed to funding acquisition, conceptualisation, supervision, and reviewing.

Ethics approval and consent to participate. The study was approved by the Cantonal Ethics Commission Zurich (BASEC 2022-01382) and conducted in accordance with the Declaration of Helsinki. All participants provided written informed consent prior to participation.

Competing interests. L.I. has received honoraria for lectures, advisory board participation, or consulting from UCB, Eisai, and Medtronic (all not related to this work). The remaining authors declare no competing interests.

Data availability. The datasets generated and analysed during this study contain potentially identifiable patient information and are therefore not publicly available. De-identified data are available from the corresponding author on reasonable request, subject to approval by the Cantonal Ethics Commission Zurich and a data-transfer agreement, in accordance with applicable data-protection regulations.

Code availability. The custom analysis code supporting the findings of this study is available from the corresponding author on reasonable request, in accordance with local ethics committee regulations.

References

[1] Luo, Y. *et al.* Global, regional, national epidemiology and trends of Parkinson's disease from 1990 to 2021: findings from the Global Burden of Disease Study 2021. *Frontiers in Aging Neuroscience* **Volume 16 - 2024** (2025). URL https://www.frontiersin.org/journals/aging-neuroscience/articles/10.3389/fnagi.2024.1498756.

[2] Poewe, W. *et al.* Parkinson disease. *Nature Reviews. Disease Primers* **3**, 17013 (2017).

[3] Groiss, S. J., Wojtecki, L., Südmeyer, M. & Schnitzler, A. Deep brain stimulation in Parkinson's disease. *Therapeutic Advances in Neurological Disorders* (2009). URL http://www.sagepub.co.uk/.

[4] Thenaisie, Y. *et al.* Principles of gait encoding in the subthalamic nucleus of people with Parkinson's disease. *Science Translational Medicine* **14**, eabo1800 (2022). URL https://www.science.org/doi/10.1126/scitranslmed.abo1800.

[5] Little, S. & Brown, P. The functional role of beta oscillations in Parkinson's disease. *Parkinsonism and Related Disorders* **20**, S44–S48 (2014). URL http://dx.doi.org/10.1016/S1353-8020(13)70013-0.

[6] Bernasconi, E. *et al.* Neurophysiological gradient in the Parkinsonian subthalamic nucleus as a marker for motor symptoms and apathy. *npj Parkinson's Disease* **11**, 1–11 (2025). URL https://www.nature.com/articles/s41531-024-00848-2.

[7] George, J. S. *et al.* Dopaminergic therapy in Parkinson's disease decreases cortical beta band coherence in the resting state and increases cortical beta band power during executive control. *NeuroImage: Clinical* **3**, 261–270 (2013). URL https://www.sciencedirect.com/science/article/pii/S2213158213001034.

[8] Bichsel, O. *et al.* Functionally separated networks for self-paced and externally-cued motor execution in Parkinson's disease: Evidence from deep brain recordings in humans. *NeuroImage* **177**, 20–29 (2018).

[9] Miron-Shahar, Y. *et al.* Excessive phase synchronization in cortical activation during locomotion in persons with Parkinson's disease. *Parkinsonism & Related Disorders* **65**, 210–216 (2019). URL https://www.prd-journal.com/article/S1353-8020(19)30251-2/fulltext.

[10] Asher, E. E. *et al.* Connectivity of EEG synchronization networks increases for Parkinson's disease patients with freezing of gait. *Communications Biology* **4**, 1–10 (2021). URL https://www.nature.com/articles/s42003-021-02544-w.

[11] Lalo, E. *et al.* Patterns of Bidirectional Communication between Cortex and Basal Ganglia during Movement in Patients with Parkinson Disease. *Journal of*

Neuroscience **28**, 3008–3016 (2008). URL https://www.jneurosci.org/content/28/12/3008.

[12] Mathiopoulou, V. *et al.* Modulation of subthalamic beta oscillations by movement, dopamine, and deep brain stimulation in Parkinson's disease. *npj Parkinson's Disease* **10**, 1–7 (2024). URL https://www.nature.com/articles/s41531-024-00693-3. Number: 1.

[13] Binns, T. S. *et al.* Shared pathway-specific network mechanisms of dopamine and deep brain stimulation for the treatment of Parkinson's disease. *Nature Communications* **16**, 3587 (2025). URL https://www.nature.com/articles/s41467-025-58825-z.

[14] Hill, M. E. *et al.* Paradoxical Modulation of STN Beta-Band Activity with Medication Compared to Deep Brain Stimulation. *Movement disorders : official journal of the Movement Disorder Society* **39**, 192 (2023). URL https://pmc.ncbi.nlm.nih.gov/articles/PMC10843006/.

[15] Pfurtscheller, G. & Lopes da Silva, F. H. Event-related EEG/MEG synchronization and desynchronization: basic principles. *Clinical Neurophysiology* **110**, 1842–1857 (1999). URL https://www.sciencedirect.com/science/article/pii/S1388245799001418.

[16] Cheyne, D., Bells, S., Ferrari, P., Gaetz, W. & Bostan, A. C. Self-paced movements induce high-frequency gamma oscillations in primary motor cortex. *NeuroImage* **42**, 332–342 (2008). URL https://www.sciencedirect.com/science/article/pii/S1053811908004965.

[17] Crone, N. Functional mapping of human sensorimotor cortex with electrocorticographic spectral analysis. II. Event-related synchronization in the gamma band. *Brain* **121**, 2301–2315 (1998). URL https://academic.oup.com/brain/article-lookup/doi/10.1093/brain/121.12.2301.

[18] Gwin, J. T., Gramann, K., Makeig, S. & Ferris, D. P. Electrocortical activity is coupled to gait cycle phase during treadmill walking. *NeuroImage* **54**, 1289–1296 (2011). URL https://www.sciencedirect.com/science/article/pii/S1053811910011638.

[19] Zhao, M. *et al.* Frequency-dependent modulation of neural oscillations across the gait cycle. *Human Brain Mapping* **43**, 3404–3415 (2022). URL https://onlinelibrary.wiley.com/doi/abs/10.1002/hbm.25856. _eprint: https://onlinelibrary.wiley.com/doi/pdf/10.1002/hbm.25856.

[20] Borhanazad, M. *et al.* Lateralized modulation of cortical beta power during human gait is related to arm swing. *iScience* **27** (2024). URL https://www.cell.com/iscience/abstract/S2589-0042(24)01526-8.

[21] Seeber, M., Scherer, R., Wagner, J., Solis-Escalante, T. & Müller-Putz, G. R. EEG beta suppression and low gamma modulation are different elements of human upright walking. *Frontiers in Human Neuroscience* **Volume 8 - 2014** (2014). URL https://www.frontiersin.org/journals/human-neuroscience/articles/10.3389/fnhum.2014.00485.

[22] Guo, X. *et al.* Neural Correlates of Abnormal Cortical Gait Control in Parkinson's Disease: A Whole-Gait-Cycle EEG Study. *IEEE Transactions on Biomedical Engineering* **71**, 400–409 (2024). URL https://ieeexplore.ieee.org/document/10207707/?arnumber=10207707. Conference Name: IEEE Transactions on Biomedical Engineering.

[23] Chung, J. W. *et al.* Beta-band oscillations in the supplementary motor cortex are modulated by levodopa and associated with functional activity in the basal ganglia. *NeuroImage: Clinical* **19**, 559–571 (2018). URL https://www.sciencedirect.com/science/article/pii/S2213158218301670.

[24] Stegemöller, E. L., Allen, D. P., Simuni, T. & MacKinnon, C. D. Motor cortical oscillations are abnormally suppressed during repetitive movement in patients with Parkinson's disease. *Clinical Neurophysiology* **127**, 664–674 (2016). URL https://www.sciencedirect.com/science/article/pii/S1388245715006094.

[25] Lofredi, R. *et al.* Beta bursts during continuous movements accompany the velocity decrement in Parkinson's disease patients. *Neurobiology of Disease* **127**, 462–471 (2019). URL https://doi.org/10.1016/j.nbd.2019.03.013.

[26] Canessa, A., Palmisano, C., Isaias, I. U. & Mazzoni, A. Gait-related frequency modulation of beta oscillatory activity in the subthalamic nucleus of parkinsonian patients. *Brain Stimulation* **13**, 1743–1752 (2020). URL https://www.sciencedirect.com/science/article/pii/S1935861X2030245X.

[27] Hell, F., Plate, A., Mehrkens, J. H. & Bötzel, K. Subthalamic oscillatory activity and connectivity during gait in Parkinson's disease. *NeuroImage. Clinical* **19**, 396–405 (2018).

[28] Quinn, E. J. *et al.* Beta oscillations in freely moving Parkinson's subjects are attenuated during deep brain stimulation. *Movement Disorders* **30**, 1750–1758 (2015). URL https://onlinelibrary.wiley.com/doi/abs/10.1002/mds.26376. _eprint: https://onlinelibrary.wiley.com/doi/pdf/10.1002/mds.26376.

[29] Scafa, S. *et al.* Activity-dependent adaptive deep brain stimulation improves gait in Parkinson's disease. *Nature Medicine* 1–16 (2026). URL https://www.nature.com/articles/s41591-026-04432-4.

[30] Jensen, O. & Mazaheri, A. Shaping Functional Architecture by Oscillatory Alpha Activity: Gating by Inhibition. *Frontiers in Human Neuroscience* **4** (2010). URL https://www.frontiersin.org/journals/human-neuroscience/

articles/10.3389/fnhum.2010.00186/full.

[31] Klimesch, W. Alpha-band oscillations, attention, and controlled access to stored information. *Trends in Cognitive Sciences* **16**, 606–617 (2012). URL https://www.sciencedirect.com/science/article/pii/S1364661312002434.

[32] Wagner, J., Makeig, S., Gola, M., Neuper, C. & Müller-Putz, G. Distinct β Band Oscillatory Networks Subserving Motor and Cognitive Control during Gait Adaptation. *Journal of Neuroscience* **36**, 2212–2226 (2016). URL https://www.jneurosci.org/content/36/7/2212.

[33] Iskhakova, L. *et al.* Modulation of dopamine tone induces frequency shifts in cortico-basal ganglia beta oscillations. *Nature Communications* **12**, 7026 (2021). URL https://pmc.ncbi.nlm.nih.gov/articles/PMC8640051/.

[34] Chu, H.-Y. *et al.* Dysfunction of motor cortices in Parkinson's disease. *Cerebral Cortex* **34**, bhae294 (2024). URL https://doi.org/10.1093/cercor/bhae294.

[35] Wang, D. D. & Choi, J. T. Brain Network Oscillations During Gait in Parkinson's Disease. *Frontiers in Human Neuroscience* 23 (2020). URL www.frontiersin.org.

[36] Stuart, S., Belluscio, V., Quinn, J. F. & Mancini, M. Pre-frontal Cortical Activity During Walking and Turning Is Reliable and Differentiates Across Young, Older Adults and People With Parkinson's Disease. *Frontiers in Neurology* **10** (2019). URL https://www.frontiersin.org/journals/neurology/articles/10.3389/fneur.2019.00536/full.

[37] Bulea, T. C., Kim, J., Damiano, D. L., Stanley, C. J. & Park, H.-S. Prefrontal, posterior parietal and sensorimotor network activity underlying speed control during walking. *Frontiers in Human Neuroscience* **Volume 9 - 2015** (2015). URL https://www.frontiersin.org/journals/human-neuroscience/articles/10.3389/fnhum.2015.00247.

[38] Fischer, P. *et al.* Alternating Modulation of Subthalamic Nucleus Beta Oscillations during Stepping. *Journal of Neuroscience* **38**, 5111–5121 (2018). URL https://www.jneurosci.org/content/38/22/5111.

[39] Louie, K. H. *et al.* Cortico-Subthalamic Field Potentials Support Classification of the Natural Gait Cycle in Parkinson's Disease and Reveal Individualized Spectral Signatures. *eNeuro* **9** (2022). URL https://www.eneuro.org/content/9/6/ENEURO.0325-22.2022. Section: Research Article: New Research.

[40] Giannicola, G. *et al.* The effects of levodopa and ongoing deep brain stimulation on subthalamic beta oscillations in Parkinson's disease. *Experimental Neurology* **226**, 120–127 (2010). URL https://www.sciencedirect.com/science/article/pii/S0014488610002931.

[41] Louie, K. H. *et al.* Adaptive deep brain stimulation for dynamic gait control in Parkinson's disease: a randomized feasibility trial. *Nature Medicine* (2026). URL https://www.nature.com/articles/s41591-026-04434-2.

[42] Gyurkovics, M., Clements, G. M., Low, K. A., Fabiani, M. & Gratton, G. The impact of 1/f activity and baseline correction on the results and interpretation of time-frequency analyses of EEG/MEG data: A cautionary tale. *NeuroImage* **237**, 118192 (2021). URL https://linkinghub.elsevier.com/retrieve/pii/S1053811921004699.

[43] Mei, Z. *et al.* Cortical and Subthalamic Dynamics Associated with Distinct Gait Domains in Parkinson's Disease (2026). URL https://www.researchsquare.com/article/rs-10770297/v1.

[44] Nasreddine, Z. S. *et al.* The Montreal Cognitive Assessment, MoCA: a brief screening tool for mild cognitive impairment. *Journal of the American Geriatrics Society* **53**, 695–699 (2005).

[45] Salzmann, L. *et al.* Synchronizing EEG with Intracranial DBS Electrode Recordings for Neurophysiological Research (2026). URL https://www.medrxiv.org/content/10.64898/2026.07.29.26358654v1. ISSN: 3067-2007 Pages: 2026.07.29.26358654.

[46] Jas, M., Engemann, D. A., Bekhti, Y., Raimondo, F. & Gramfort, A. Autoreject: Automated artifact rejection for MEG and EEG data. *NeuroImage* **159**, 417–429 (2017). URL https://linkinghub.elsevier.com/retrieve/pii/S1053811917305013.

[47] Pion-Tonachini, L., Kreutz-Delgado, K. & Makeig, S. ICLabel: An automated electroencephalographic independent component classifier, dataset, and website. *NeuroImage* **198**, 181–197 (2019). URL https://pmc.ncbi.nlm.nih.gov/articles/PMC6592775/.

[48] O'Connor, C. M., Thorpe, S. K., O'Malley, M. J. & Vaughan, C. L. Automatic detection of gait events using kinematic data. *Gait & Posture* **25**, 469–474 (2007).

[49] Alijanpour, E. & Russell, D. M. Gait phase normalization resolves the problem of different phases being compared in gait cycle normalization. *Journal of Biomechanics* **173**, 112253 (2024). URL https://www.sciencedirect.com/science/article/pii/S0021929024003312.

[50] Donoghue, T. *et al.* Parameterizing neural power spectra into periodic and aperiodic components. *Nature Neuroscience* **23**, 1655–1665 (2020). URL https://www.nature.com/articles/s41593-020-00744-x.

[51] Gerster, M. *et al.* Separating Neural Oscillations from Aperiodic 1/f Activity: Challenges and Recommendations. *Neuroinformatics* **20**, 991–1012 (2022). URL https://doi.org/10.1007/s12021-022-09581-8.

[52] Benjamini, Y. & Hochberg, Y. Controlling the False Discovery Rate: A Practical and Powerful Approach to Multiple Testing. *Journal of the Royal Statistical Society. Series B (Methodological)* **57**, 289–300 (1995). URL https://www.jstor.org/stable/2346101.

Supplementary information. Supplementary information is available with the online version of this paper.

Supplementary Files

This is a list of supplementary files associated with this preprint. Click to download.

- Supplementary.pdf